Anisotropic Coarsening of Two-Dimensional Surface Domains in Copolymer Thin Films

Jakob Heier, Easan Sivaniah, and Edward J. Kramer*

Materials Department, University of California at Santa Barbara, Santa Barbara, California 93106

Received June 8, 1999; Revised Manuscript Received October 18, 1999

ABSTRACT: We have investigated by scanning force microscopy the growth of surface relief structures on thin diblock copolymer films for a $\infty \times \infty$ geometry (homogeneous substrate) and a $L \times \infty$ geometry (heterogeneous substrate). We characterize the growth by a length scale obtained from the correlation function describing the fluctuations. Two-dimensional viscous flow within a continuous layer dominates the process. On the homogeneous substrate we find a power law growth with an exponent of $\alpha = {}^2/_3$, while the growth on the stripe pattern in a direction parallel to the stripes is characterized by an exponent that is much lower.

Introduction

Phase separation phenomena leading to two coexisting phases have attracted attention for more than a century.[1−3] However, initially the phase separating system is not necessarily in equilibrium. The total free energy of the system can be lowered by decreasing the total interfacial energy. These very late stages of spinodal decomposition or nucleation and growth are usually referred to as coarsening or Ostwald ripening.[4] Similarly, surface domains (islands or holes) in thin diblock copolymer films coalesce, driven by the line tension of the surface domains. Generally, in symmetric block copolymer thin films, the interaction of the blocks with the interfaces induces an orientation of lamellar microdomains parallel to the surface. As a consequence, if the film does not possess a certain quantized film thickness, the film will decompose into a film with two coexisting equilibrium film thicknesses. For example, in a thin film of a symmetric poly(styrene-*b*-vinylpyridine) (PS−PVP) diblock copolymer on a polar surface, the PVP block is expected to be located at the substrate/polymer interface while PS lies at the air/polymer interface. Stable flat film thicknesses can be found only for films with an initial thickness of $(m + {}^1/_2)L_0$, where L_0 is the lamellar period and m is an integer. A film with an initial thickness of mL_0 will decompose into a film with an equal area of the two coexisting thicknesses $(m - {}^1/_2)L_0$ and $(m + {}^1/_2)L_0$. The surface domain pattern resulting from this process resembles a bicontinuous spinodal decomposition pattern in two dimensions. In this picture higher film sections correspond to phase A and lower film sections to phase B, or vice versa. For thicknesses larger or smaller than mL_0, a hole structure or island structure, respectively, is formed. Coarsening becomes more complex under the influence of absorbing walls as we expect a complicated interplay of domain growth and wetting layer growth.[5] When the size of the domains becomes comparable to the distances between the walls, finite size effects may come into play.[6,7]

In recent experiments we demonstrated that, by annealing films on substrates patterned by a grating consisting of alternating stripes of H_3C- and HO-terminated self-assembled monolayers (SAMs), the film above the H_3C−SAM attracts and absorbs excess material and thus produces absorbing boundary conditions at the boundary with the HO−SAM. Island formation on a HO−SAM striped substrate thus effectively takes place in a $L \times \infty$ geometry. We present here the results of new experiments on the late stage coarsening of surface domains confined between H_3C−SAM stripes.

Experimental Section

The block copolymers being investigated are symmetric poly(styrene-*b*-2-vinylpyridine) (PS−PVP) diblock copolymers. The polymers were synthesized by anionic polymerization.[8] The indices of polymerization of the PS and PVP blocks are $N_{PS} = 960$ and $N_{PVP} = 960$. The Flory interaction parameter $\chi = -0.033 + 63/T$.[9] At an annealing temperature of $T = 176$ °C, a temperature chosen to be well above the glass transition temperature T_g (110 °C of both the PS and the PVP blocks), the system is well inside the strong segregation regime and forms a lamellar morphology. We determined the equilibrium lamellar thickness in bulk samples via cross-sectional transmission electron microscopy (TEM) and in thin films via scanning force microscopy (SFM) by determining the height of islands and holes forming on the surface. We obtain good agreement between the two methods and find the lamellar period to be $L_0 = 69$ nm. Patterned self-assembled monolayers (SAMs) were formed by a microcontact printing technique.[10] Stripes of H_3C-terminated thiols were transferred onto an Au film substrate by a microfabricated elastomer stamp. The gold is about 200 nm thick and was freshly evaporated by an e-gun evaporator onto a silicon substrate covered by a 10 nm thick chromium adhesive layer. Subsequently, the substrate was immersed into a solution of HO-terminated thiols, allowing monolayers to form in the empty spaces between the lines of the H_3C-terminated SAM. In this way we produced gratings with periodicities varying from 6 to 20 μm. The ratio of the width of the HO−SAM stripe to the H_3C−SAM is 3:1: We consider in more detail periodicities of 16, 12, and 8 μm. For these periodicities the HO−SAM stripe widths are 12, 9.2, and 6 μm, respectively. The H_3C−SAM stripe widths are 4, 2.8, and 2 μm, respectively. PS−PVP films of 138 nm thickness ($2.0L_0$) were spun-cast onto the patterned sub strates from toluene solutions. Annealing was done in a high-vacuum furnace (7×10^{-5} Pa) at a temperature of 176 °C. The topography was imaged with a di-Dimension 3000 scanning force microscope (SFM) from Digital Instruments (Santa Barbara). We used a Si_3N_4 tip on a cantilever with a nominal force constant of 0.06 N m^{-1} in constant force mode.

* To whom correspondence should be addressed.

10.1021/ma990916u CCC: $18.00
Published on Web 12/08/1999

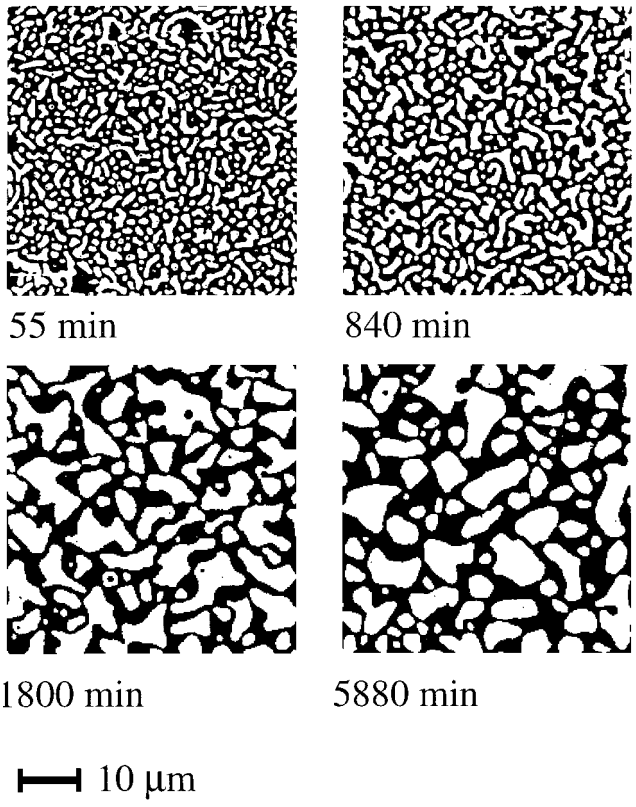

Figure 1. SFM micrograph of the time evolution of a PS−PVP film slightly thicker than $2.0L_0$ on a homogeneous HO−SAM. The base side of the SFM scans is 50 μm. White areas are film sections that are $1.5L_0$ in height, and black areas are $2.5L_0$ in height.

Results

In what follows we investigate films that are slightly thicker than $2.0L_0$. Stable flat films would be achieved for initial film thicknesses of $1.5L_0$ and $2.5L_0$ with a PVP domain against the substrate and a PS domain against the vacuum surface of the copolymer. We first investigate the domain coarsening on a homogeneous substrate. Figure 1 shows the time evolution of a PS−PVP film slightly thicker than $2.0L_0$ annealed at 176 °C on a HO-terminated SAM. After a short annealing time a hole pattern of $1.5L_0$ thick areas within a $2.5L_0$ thick film develops (Figure 1, 55 min).

The coarsening process is dominated by the growth of larger holes at the cost of smaller ones. But even for long annealing times (Figure 1, 5880 min) a bimodal size distribution of holes exists. We now compare these results with the behavior of a $2.0L_0$ thick PS−PVP film annealed on a patterned substrate. Figure 2 shows a SFM image of a PS−PVP film after 20 h of annealing at 176 °C on a set of H_3C/HO−SAM stripes with a period of 16 μm (HO−SAM stripe width 12 μm and H_3C−SAM stripe width 4 μm). Above the HO−SAM the two thicknesses $1.5L_0$ and $2.5L_0$ coexist, while on top of the H_3C−SAM a complete layer is formed that seems to be not restricted by thickness quantization.

In our earlier work we demonstrated that a film above the H_3C−SAM shows a poor alignment of lamellae parallel to the substrate.[11] Accumulation of excess copolymer is more favorable on defect-rich lamellae compared to a defect-free lamellar film. This poor alignment of the film above the H_3C−SAM is thus the reason why this polymer layer produces absorbing boundary conditions. We will show later on that the height of this layer increases with time.

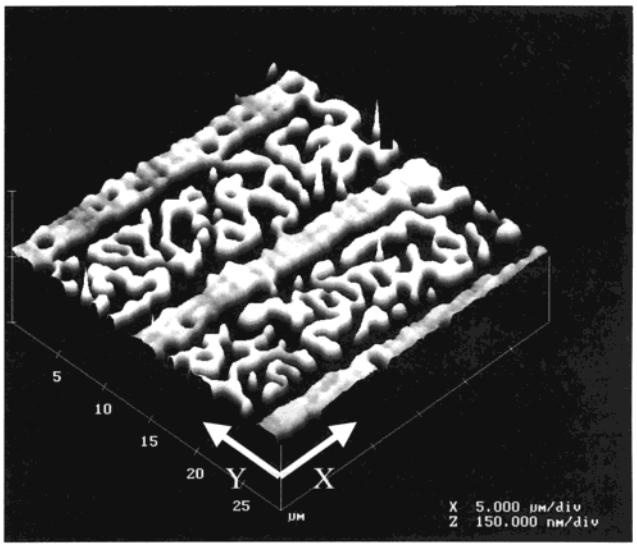

Figure 2. Pattern formation on a $2.0L_0$ thick PS−PVP film on a HO/H_3C−SAM pattern with a HO−SAM stripe width of 8 μm and a H_3C−SAM stripe width of 4 μm. The sample was annealed at 176 °C for 100 min, and the evolving topography was imaged by SFM. The H_3C−SAM stripes are covered by an almost complete layer of PS−PVP, while the HO−SAM stripe hosts the two coexisting thicknesses $1.5L_0$ and $2.5L_0$.

Figures 3−5 show the temporal evolution of the pattern for HO−SAM stripe widths of 12, 9.2, and 6 μm. Regions above the HO−SAM that are $2.5L_0$ in height are marked in black and those that are $1.5L_0$ in height are white; the "sink" above the H_3C−SAM is also marked in black, even though its thickness changes with time. After very short annealing times we find a nearly continuous trench, whose bottom is $1.5L_0$ above the substrate, inside the HO−SAM and adjacent to the H_3C−SAM. This material has been absorbed by the film above the H_3C−SAM after being transported over the shortest possible distance. This transport happens during the very early stages of microphase separation and while the lamellae are being aligned parallel to the substrate. Thus, the trench formation occurs simultaneously with the initial ordering and is not a consequence of the late stage coarsening process. Further inside the HO−SAM stripe, a stripe rich in elevated areas develops (an "enrichment layer" next to the "depletion zone").

For short annealing times we find a bicontinuous structure in the center of the HO−SAM stripe. Upon further annealing these features coarsen, and they do so in a characteristic manner: We observe neither the dissolution of isolated islands nor the diffusion of isolated whole islands along the surface. We do not find evidence for material flow across the "depletion zone" into the absorbing boundaries, but we do observe material flowing through bridges from domain structures into the area of the boundary. This observation becomes most obvious for the gratings with smaller periodicity (Figure 5). In many cases the copolymer layer on the H_3C−SAM is higher next to these bridges. The size of isolated islands does not change in time. The dominating process is two-dimensional pressure driven flow within an interconnected domain structure. The observation that isolated islands seem to be pinned to their original positions is also supported by our experiments on thinner films (where we find only isolated islands but no interconnected domains). Here islands eventually dissolve, but only after much longer anneal-

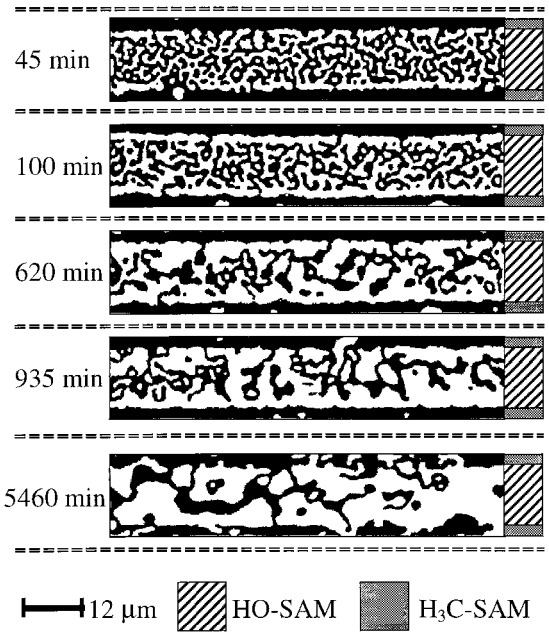

Figure 3. Time evolution of a single period of a grating with 16 μm periodicity (HO−SAM stripe width is 12 μm). The $2.0L_0$ thick PS−PVP film was annealed at 176 °C. Each stripe is 70 μm long, and we show one full period in width (the HO−SAM stripe and half a H_3C−SAM stripe on each side).

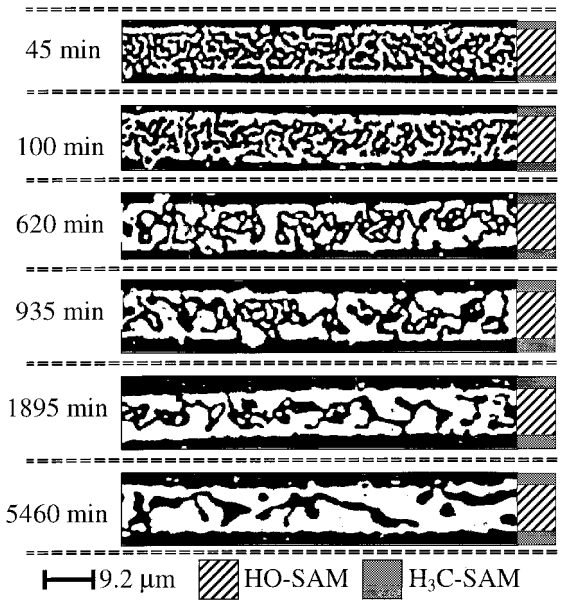

Figure 4. The same as in Figure 3 for a grating periodicity of 12 μm (and an HO−SAM stripe width of 9.2 μm).

ing times and only close to absorbing walls.

The difference in kinetics between isolated islands and interconnected domains is a consequence of the topological structure inside the domains. We depict these differences in Figure 6. In the case of a hole within a complete layer, the bilayers around the defect structure (the hole) are continuous, while for an isolated island on top of a complete layer, one bilayer is trapped within the island. For a hole (or a bicontinuous structure) matter can simply be exchanged by two-dimensional flows within the same layer. For an isolated island to exchange copolymer chains, single molecules either have to diffuse across the surface or move into the underlying coherent polymer layer. For the first scenario, the PVP block of a single chain is exposed to

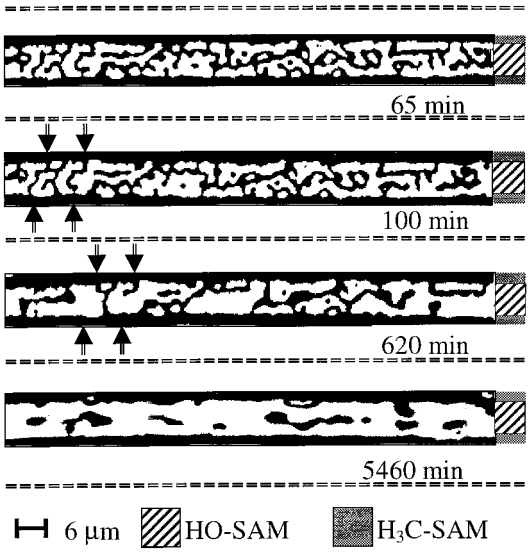

Figure 5. The same as in Figure 3 for a grating periodicity of 8 μm (HO−SAM stripe width 6 μm). The arrows mark examples of H_3C−SAM boundary sections that absorb polymer from the HO−SAM film section.

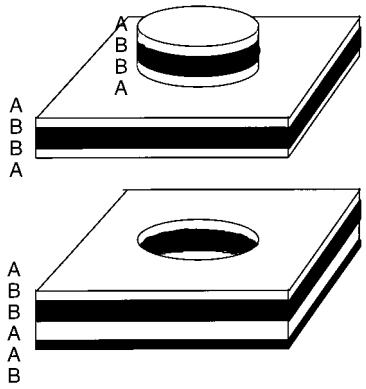

Figure 6. Schematic sketch of an idealized domain edge structure for an island and a hole. The real edge structure is more complicated, as the B-block does not want to be exposed to the vacuum surface but at the same time the block structure of the polymer imposes geometrical constraints onto the system.

air, which is energetically unfavorable. For the second scenario the PVP block has to flow through the defect structure at the edge of an island. Thus, islands are much more stable than holes or a network structure.[12]

The coarsening process is not self-similar as we anticipate immediately from the SFM scans. The domains have an elongated shape and are aligned parallel to the H_3C/HO−SAM interface. Figures 7 and 8 show laterally averaged height profiles corresponding to the evolution depicted in Figures 4 and 5. The profiles are obtained by averaging the height profile scanned along the *y*-axis over scans equally spaced in the *x*-direction (parallel to the grating). The height of the so-averaged copolymer layer on top of the H_3C−SAM increases continually with time, indicating that the copolymer above the H_3C−SAM has absorbing character throughout the whole process. In the next section we focus our attention on the HO−SAM stripes.

For HO−SAM stripes of 12 and 9.2 μm width, a height profile that oscillates with a characteristic wavelength is present throughout the whole sample at early times but not at later times. At a later stage we only have one distinct minimum next to the absorbing wall while

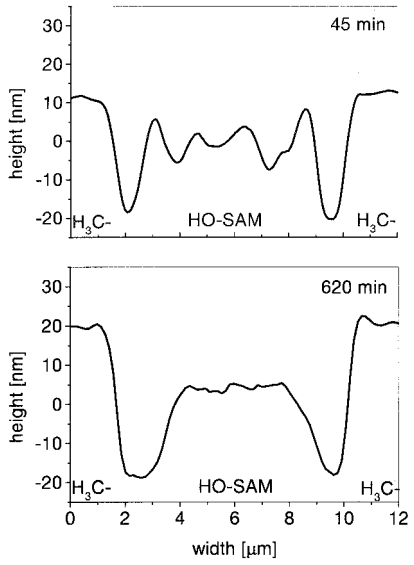

Figure 7. Averaged height of the surface domains on the HO−SAM as a function of distance from the HO/H_3C−SAM boundary for the grating with an HO−SAM stripe width of 9.2 μm. These profiles are an average of *y*-scans equally spaced along a 75 μm length of the HO−SAM stripe in the *x*-direction. The axes *x* and *y* are defined in Figure 2.

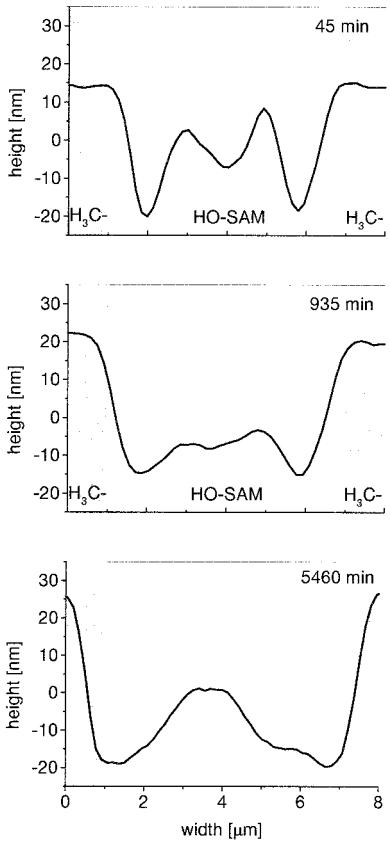

Figure 8. Averaged height of the surface domains on the HO−SAM as a function of distance from the HO/H_3C−SAM boundary for the grating with an HO−SAM stripe width of 6 μm. These profiles are an average of *y*-scans equally spaced along a 75 μm length of the HO−SAM stripe.

the center of the stripe resembles the height profile of a homogeneous substrate, where the height features are randomly oriented and a similar averaging gives rise to a featureless profile. For HO−SAMs of 6 μm width, the oscillations originating from both of the HO/H_3C−SAM boundaries interfere and give rise to a height profile that evolves from a height profile with two peaks to a featureless profile (destructive interference) and finally to a domain structure with one center peak in the middle of the stripe. The initial ordering favors certain positions of excess islands due to a spinodal process.[13]

With this picture in mind we can reassess the observations made in Figure 5. For short annealing we find most of the excess polymer to be located in two stripes, each about 2 μm away from the nearest H_3C/HO−SAM interface. Upon further annealing domains are either absorbed from the wall or merge into the domains that remain in the center of the stripe. The depletion zone adjacent to the wall grows, and most of the excess polymer assembles within one elongated domain which is only weakly localized around the center of the stripe.

We now compare these results to our earlier experiments, obtained from samples with a lower surface coverage. Here we observed a large-amplitude pattern over the HO−SAM when the stripe width is $D = \lambda/2$, $(3/2)\lambda$, and $(5/2)\lambda$ (constructive interference from the waves originating from opposite interfaces) and a low-amplitude pattern for $D = \lambda$ and 2λ. As mentioned before, in a comparable time period we do not observe noticeable island coalescence or coarsening. To characterize the time evolution of the pattern coarsening along the grating, we introduce a two-dimensional correlation function.[14] Correlation functions are generally helpful in characterizing the dynamics of fluctuations.

$$G(x_1 - x, y) = \langle \Phi(x_1,y)\, \Phi(x,y) \rangle - \langle \Phi \rangle^2 \qquad (1)$$

The angular brackets refer to an integration over x_1 along the grating, while *y* refers to the distance of a particular line (of width $dy = 0.15$ μm) from the H_3C/HO−SAM boundary (see Figure 2). We study the behavior of the correlation function integrated over the width *D* of the whole HO−SAM stripe $G^{int}(x_1 - x)$.

$$G_{int}(x_1 - x) = \int_0^D G_1(x_1 - x, y)\, dy/D \qquad (2)$$

We denote $L_{||}$ as the distance over which the correlation function decays to half of its maximum value. We test the concept of dynamic scaling by plotting a normalized correlation function $G_{||}(X)/G_{||}(0)$ versus $X/L_{||}$ for different times, where $X = x_1 - x$. We show this normalized correlation function in Figure 9 for the homogeneous substrate (a) and HO−SAM stripes of 12 μm width (b). The function develops a characteristic minimum which can be understood as the hallmark of a spinodally decomposing system.[15−18]

For the isotropic case, the experimental data collapse onto two separate master curves depending on annealing time. After an intermediate annealing time (840 min) we observe a marked transition from a pronounced minimum at $X/L_{||} = 3.7$ in the correlation function to a less pronounced minimum at $X/L_{||} = 5$. This change reflects the fact that the process is not self-similar, as already apparent by inspection of the real space images.

In contrast, the correlation functions for the domain coarsening on a patterned substrate possess the shape of the isotropic case only for the very shortest annealing time. Upon annealing the minimum becomes less and less pronounced until the functions show a monotonic decay to zero. For the longer annealing times, dynamic scaling appears to be restored, and all late-stage curves

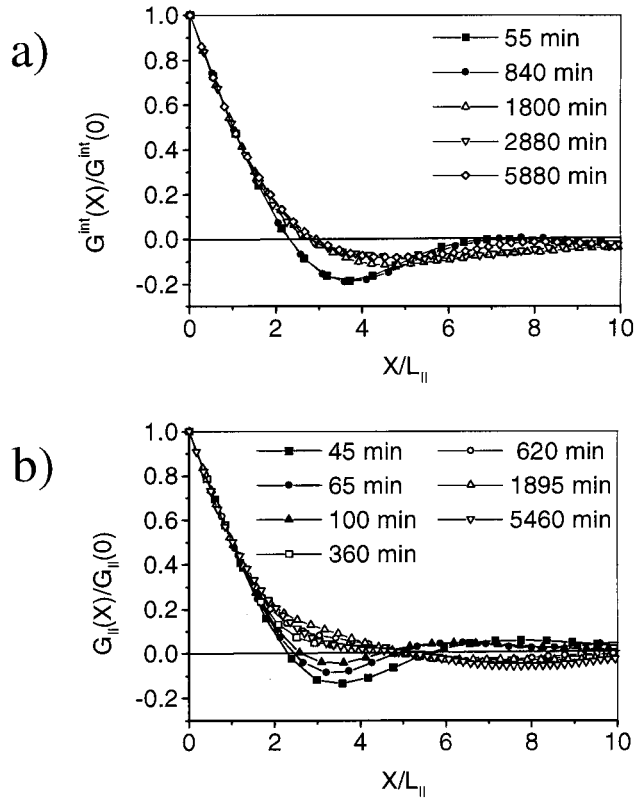

Figure 9. Integrated correlation functions $G^{int}(x,t)$ (eq 2) normalized by their maximum values $G^{int}(0,t)$ and plotted against the scaled variable $X/L_{||}$ for (a) the homogeneous substrate (as depicted in Figure 1) and (b) for the grating with an HO−SAM stripe width of 9.2 μm (as depicted in Figure 4). The functions are obtained by averaging over 5−7 HO−SAM stripes.

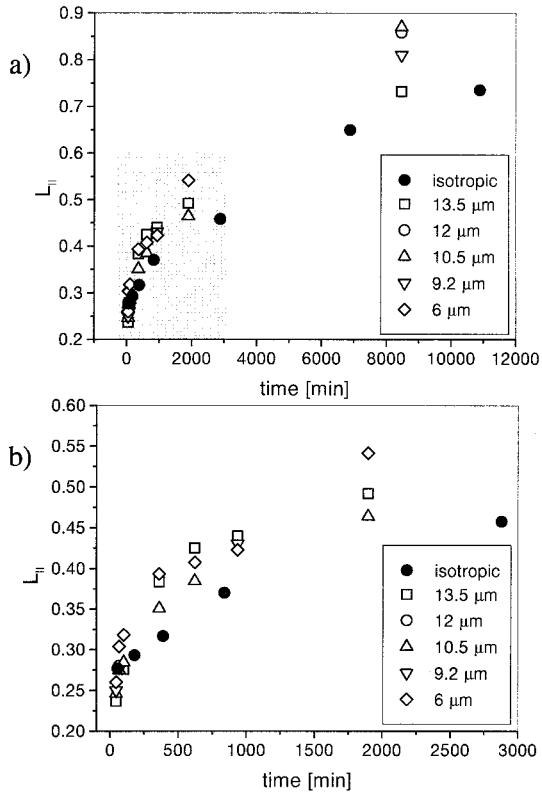

Figure 10. Time dependence of the length scale $L_{||}(t)$ for copolymer films annealed on an homogeneous samples and patterned surfaces with stripe widths of 13.5, 12, 10.5, 9.2, and 6 μm. In (b) we show the region shaded in gray from (a).

Table 1. Parameters Describing the Growth Law of the PS−PVP Films Annealed on a Homogeneous Substrate and Patterned Substrates with HO−SAM Width of 13.5, 10.5, 9.2, and 6 μm[a]

HO−SAM stripe width (μm)	a (μm)	B	α	SD
∞	0.26	0.0015	0.63	0.036
13.5	0	0.12	0.19	0.014
10.5	0.12	0.05	0.28	0.022
9.2	0.10	0.05	0.30	0.028
6	0.08	0.11	0.17	0.014

[a]All data follow the general form $L_{||} = a + bt^{\alpha}$. We also report the standard deviation (SD) of the best linear fit.

nearly fall onto one master curve. The time evolution of the characteristic linear dimension $L_{||}$ is shown in Figure 10. All data follow the general form $L_{||} = a + bt^{\alpha}$. We perform a standard linear regression analysis on linearized scales (log−log presentation). The results of this procedure are presented in Table 1. The parameters describing the samples annealed on striped surfaces differ significantly from the sample annealed on a homogeneous substrate. The initial domain size a and the growth exponent α are larger for the isotropic samples. That seems inconsistent with the observation of elongated domains along the gratings. The explanation can be found in the prefactor b, which is orders of magnitude larger for the samples on stripe patterns.

Discussion

In this study we present experimental results on late stage pattern coarsening in a thin diblock copolymer film, where a region forming islands is laterally confined between walls that absorb copolymer chains. This is an ideal model system to study late stage coarsening processes in two dimensions as the process can be monitored easily in real space with scanning force microscopy techniques. With a microcontact printing technique we prepare film sections that produce absorbing boundary conditions with one dimension comparable to the coarsening domains. The $L \times \infty$ geometry has proven to be of special interest for theoretical considerations.[19,20] Usually real space images are not easily accessible. For example, our knowledge of decomposing polymer blend films depends on laterally averaged depth profiles and computer simulations. Also, results from these real systems are rather hard to interpret since wetting phenomena complicate the process. In this sense our boundary conditions are easier to understand. Our experiments indicate that the film above the H_3C−SAM absorbs material continuously and that the absorption process is not the rate-limiting step. Especially for the smaller gratings, absorption by the H_3C/HO−SAM boundary clearly competes with domain coarsening. For the larger periodicities the stripe area covered by domains remains constant. We suggest that hydrodynamics is the most important factor determining the coarsening. This is different from what is usually reported in the context of diblock copolymer island coarsening. Most reports describe a situation with a lower surface coverage of domains. This case does not allow for hydrodynamic flow within the surface layer. Coarsening then can only happen through diffusion of islands as a whole or through hydrodynamic flow in a coherent layer underneath the surface layer, driven by two-dimensional pressure relaxation inside this layer. This process requires single copolymer chains to move

from one layer into another layer and is thus much slower than rearrangements within the same lamellar layer. As a consequence, as soon as the islands on top of the HO−SAM are separated from the absorbing film above the H_3C−SAM, coarsening is laterally confined along the HO−SAM stripe, and we find elongated surface domains.

We shall conclude by comparing our growth exponents to values reported in the literature. For hydrodynamic flow, in a three-dimensional coarsening mixture of incompressible fluids the theoretical time exponent is $\alpha = 1$ (viscosity controlled).[21−23] In two dimensions the corresponding exponent for the viscosity controlled case changes to $\alpha = {}^1/_2$. We do not find agreement between the theory and our experiments. Instead, the exponent we determine experimentally for a homogeneous substrate lies between the values of α for the two-dimensional and three-dimensional cases.

Acknowledgment. We gratefully acknowledge primary funding for this work from the NSF-DMR-Polymers Program under Grant DMR-9803738. This work made use of MRL Central Facilities supported by the National Science Foundation under Award DMR96-32716. We thank M. Chaudhury for supplying the HO-terminated thiols used to form the HO-terminated SAM. Part of this work was performed at the Cornell Nanofabrication Facility (a member of the National Nanofabrication Users Network), which is supported by the National Science Foundation under Grant ECS-9319009, Cornell University, and industrial affiliates.

References and Notes

(1) Gunton, J. D.; San Miguel, M.; Sahni, P. S. In *Phase Transitions and Critical Phenomena;* Comb, C., Lebowitz, J. L., Eds.; Academic Press: London, 1993; Vol. 8.
(2) Komura, S., Furukawa, H., Eds. *Dynamics of Ordering Processes in Condensed Matter;* Plenum Press: New York, 1988.
(3) Binder, K. In *Materials Science and Technology;* Cahn, R. W., Haasen, P., Kramer, E. J., Eds.; VCH: Weinheim, 1991; Vol. 5.
(4) Voorhees, P. W. *J. Stat. Phys.* **1985,** *38*, 231.
(5) For reviews, see: Dietrich, S. In *Phase Transitions and Critical Phenomena;* Comb, C., Lebowitz, J. L., Eds.; Academic Press: London, 1993; Vol. 12, p 1.
(6) Barber, M. N. In *Phase Transitions and Critical Phenomena;* Domb, C., Lebowitz, J. L., Eds.; Academic Press: New York, 1983; Vol. 8, p 156.
(7) Binder, K. *Annu. Rev. Phys. Chem.* **1992,** *43*, 33.
(8) Matasushita, Y.; Shimizu, K.; Nakao, Y.; Choshi, H.; Noda, I.; Nagasawa, M. *Polym. J.* **1986,** *18*, 361.
(9) Dai, K. H.; Kramer, E. J. *Polymer* **1994,** *35*, 157. Kumar, A.; Whitesides, G. M. *Langmuir* **1991,** *7*, 1013.
(10) Kumar, A.; Whitesides, G. M. *Langmuir* **1991**, *7*, 1013.
(11) Heier, J.; Kramer, E. J.; Walheim, S.; Krausch, G. *Macromolecules* **1997,** *30*, 6610.
(12) Ausserré, D.; Chatenay, D.; Coulon, G.; Collin, B. *J. Phys. (Paris)* **1990**, *51*, 2571.
(13) Heier, J.; Genzer, J.; Kramer, E. J.; Bates, F. S.; Krausch, G. *J. Chem. Phys.*, in press.
(14) Puri, S.; Binder, K. *Phys. Rev. A* **1992,** *46***,** R4487; *Phys. Rev. E* **1994,** *49*, 5359.
(15) Huse, D. *Phys. Rev. B* **1986,** *34*, 7845.
(16) Oono, Y.; Puri, S. *Phys. Rev. Lett.* **1987**, *58*, 836. Oono, Y.; Puri, S. *Phys. Rev. A* **1988,** *38*, 434. Puri, S.; Oono, Y. *Phys. Rev. A* **1988,** *38*, 1542.
(17) Rogers, T. M.; Elder, K. K.; Desai, R. C. *Phys. Rev. B* **1988,** *37*, 196. Chakrabarti, A.; Gunton, J. D. *Phys. Rev. B* **1988,** *37*, 3798.
(18) Amar, J. G.; Sullivan, F. E.; Mountain, R. D. *Phys. Rev. B* **1988,** *37*, 196.
(19) Barber, M. N. In *Phase Transitions and Critical Phenomena*; Domb, C., Lebowitz, J. L., Eds.; Academic: New York, 1983; Vol. 8, p 145.
(20) Nightingale, M. P. In *Finite Size Scaling and Numerical Simulations of Statistical Systems*; Privman, V., Ed.; World Scientific: Singapore, 1990; pp 287−352.
(21) Siggia, E. D. *Phys. Rev. A* **1997,** *20*, 595.
(22) Furukawa, H. *Physica A* **1994,** *204*, 237.
(23) Bray, A. J. *Adv. Phys* **1994,** *43*, 357.

MA990916U